CHAPTER 3
RESULTS

The purified bioactive substance was prepared and acidified by HCl to obtain anhydronium salt. The salt was iodinated at macro and microscale by reacting with sodium iodide in the presence of oxidizing agent, chloramine-T. The [^{125}I]anhydrobarakol hydrochloride was then prepared in the same manner. All chemical structure of substances prepared in this study were confirmed by spectrophotometric methods. The [^{125}I]anhydrobarakol hydrochloride was used as a ligand to demonstrate specific binding sites by *in vitro* receptor autoradiography as follow;

1. Preparation of anhydrobarakol hydrochloride

The physical and spectroscopic characteristics of anhydrobarakol hydrochloride were evaluated; mp. 205 $^{\circ}$C (dec.); UV λ_{max} (EtOH) nm (log ε): 241 (4.8) and 398 (4.54) (Figure 5); IR ν_{max} (KBr) 3445, 1670, 1589, and 1271 cm^{-1} (Figure 6); ^{1}H-NMR (D_2O): δ 7.03 (2H,d), 6.89 (1H,b), 6.86 (1H,t), 2.71 (3H,s) and 2.48 (3H,s) (Figure 7); MS, m/z (rel.): M^+ 216 (3), 214 (100), 186 (158), 115 (11), 89 (11), 63 (9), and 51 (9) (Figure 8). These data were similar to those demonstrated by the previous works of Bycroft (1970) and Kaokaew (1993) (Table 2). The yield of the products are 70 percent.

2. Iodination reaction of anhydrobarakol hydrochloride.

The reaction between anhydrobarakol hydrochloride and sodium iodide in the presence of chloramine - T produced yellow brown precipitations which were then purified by column chromatographic technique. Spectroscopic characteristics of the collected fraction were identified as follow; UV λ_{max} (EtOH) nm (log ε): 246 (4.87) and

Table 2 Spectroscopic characteristics of anhydrobarakol hydrochlorid.

Type of spectrum	Anhydrobarakol hydrochloride (Bycrof, 1970)	Anhydrobarakol hydrochloride (Kaokeaw,1993)	Anhydrobarakol hydrochloride (Present study)
UV λ_{MAX} nm (log ε)	in H_2O 241 and 472	in EtOH 240(4.96),384(4.54)	inEtOH 241(4.8), 398(4.52)
IR ν_{max} (cm^{-1})	in Nujor 3500, 3440, 1660, 1620	in KBr 3500, 2740, 1600, 1442	In KBr 3445, 1670, 1589, 1271
NMR δ value (ppm)	in D_2O at 100 MHz 6.90 (4*1 H) 2.48, 2.70 (6H, 2* s, 2*Me)	in D_2O at 200 MHz 6.8(2*1 H), 6.60(1H), 6.40(1H), 2.47, 2.33 (6H,2*s, 2*Me)	in D_2O at 500 MHz 7.03(2 H,d), 6.89(1H,b), 6.86 (1H,t), 2.71(3H,s), 2.48 (3H,s)
Mass spectra (m/z)	M^+ 232(2), 214(100), 186(78), 158(23), 143 (6), 110(17), 93(10), 89(10), 51(13)	M^+ 232(>1), 214(98), 186(69), 158(26), 143 (8), 115(23), 93(20), 89(16), 51(19), 43(100)	M^+ 216(3), 214(100), 186(69), 158(32), 115 (11), 89(11), 63(9),51 (9)

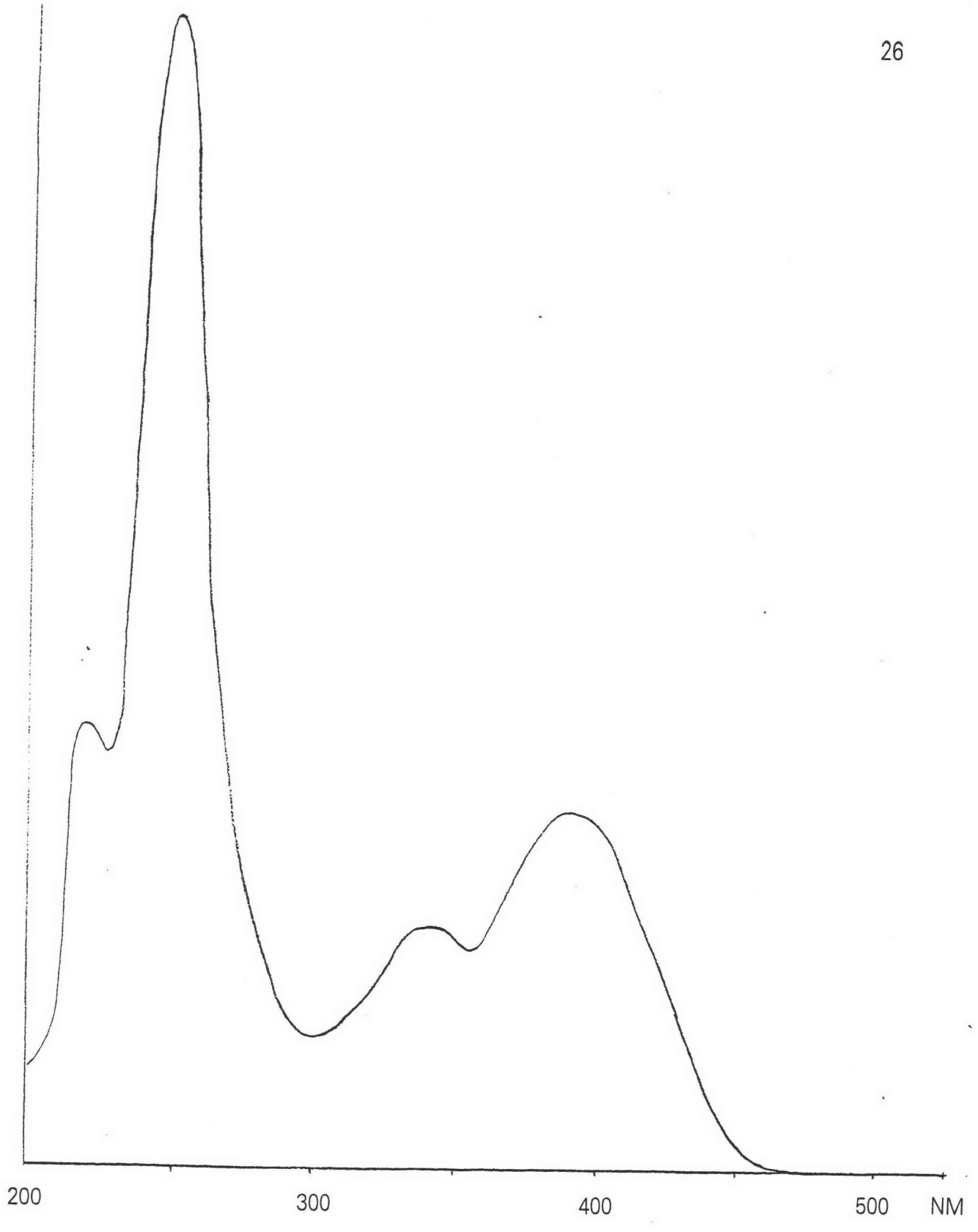

Figure 5 : UV absorption spectrum of anhydrobarakol hydrochloride.

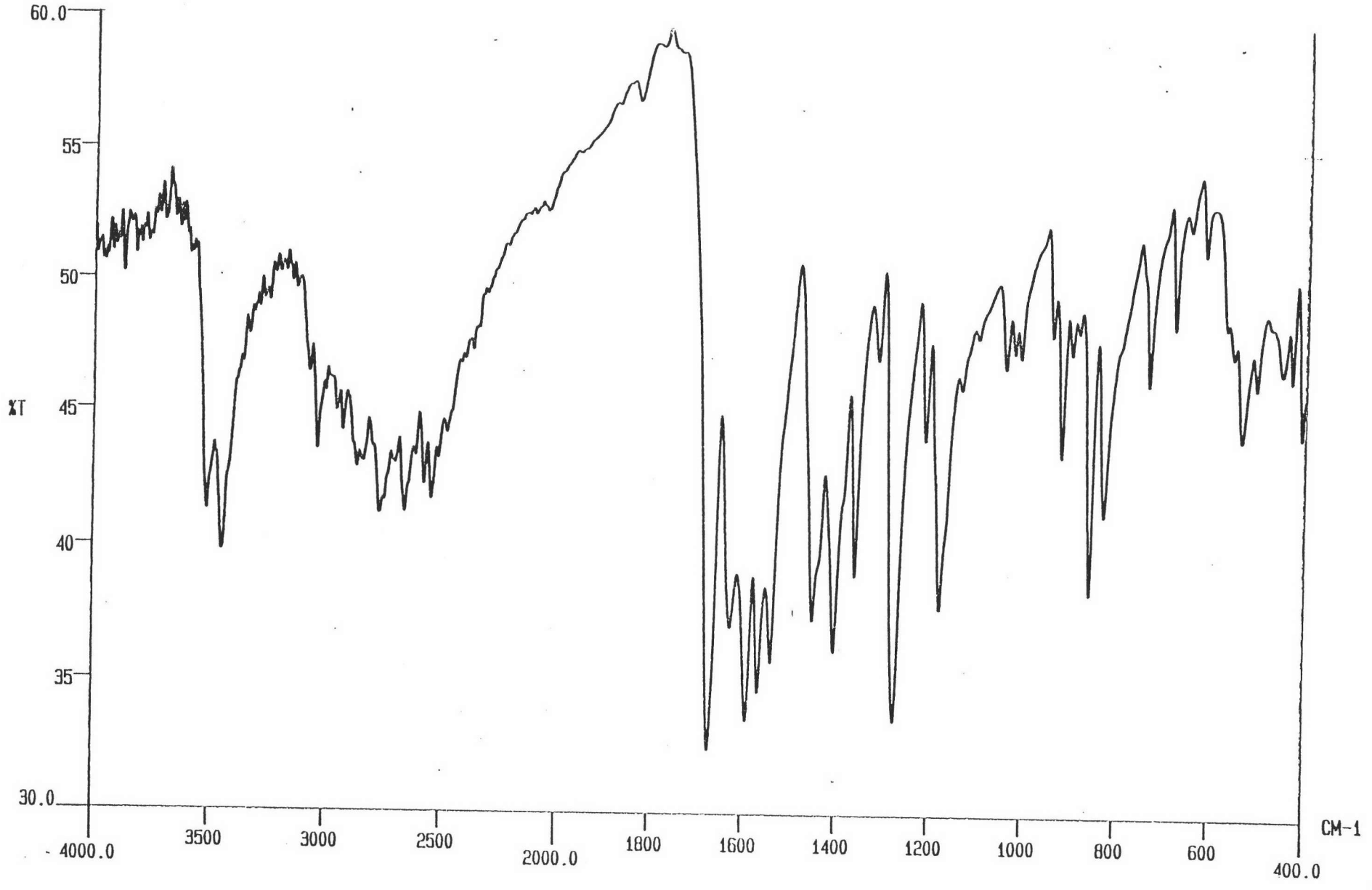

Figure 6 : IR absorption spectrum of anhydrobarakol hydrochloride, in KBr.

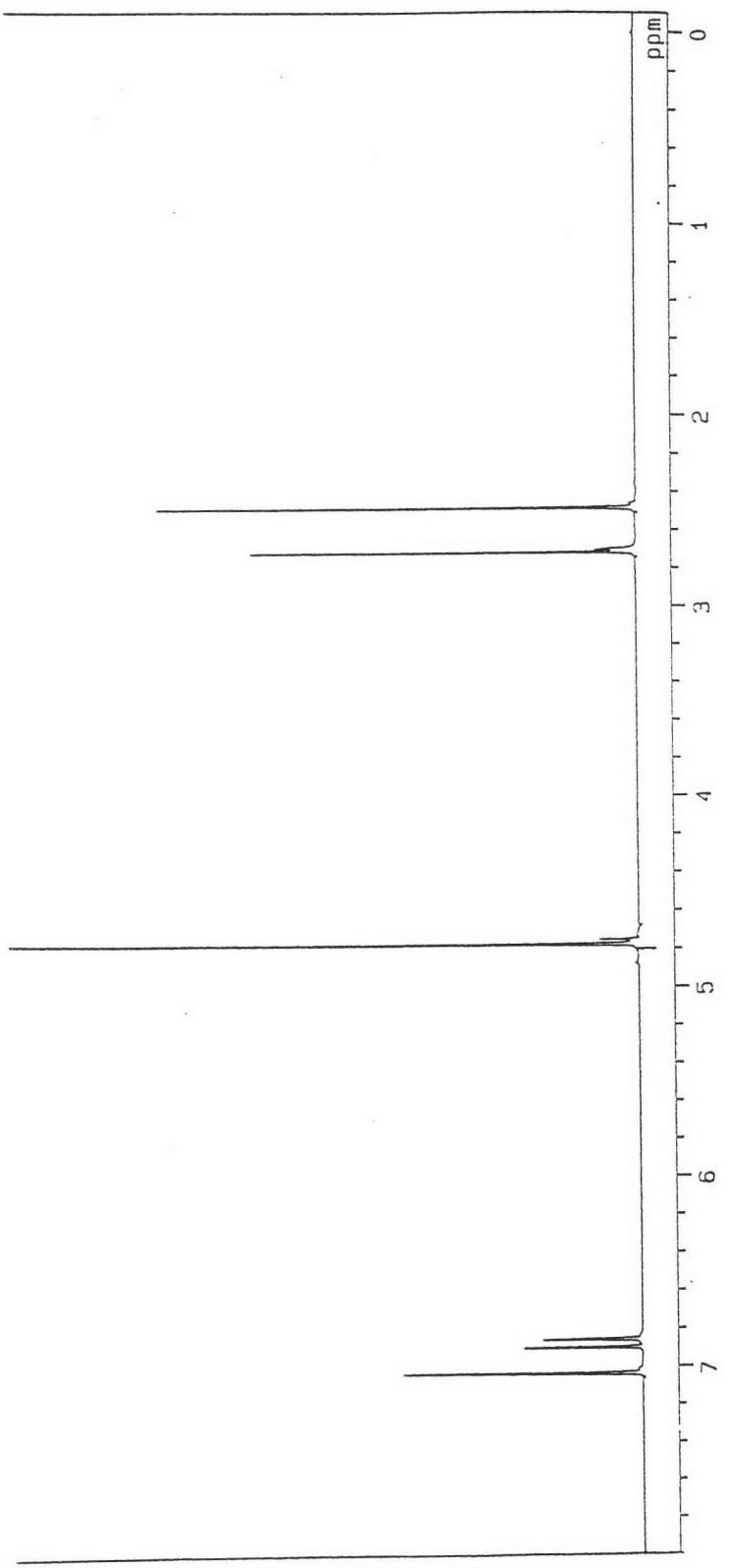

Figure 7 : ^{1}H NMR spectrum of anhydrobarakol hydrochloride, in D_2O (at 200 MH_z).

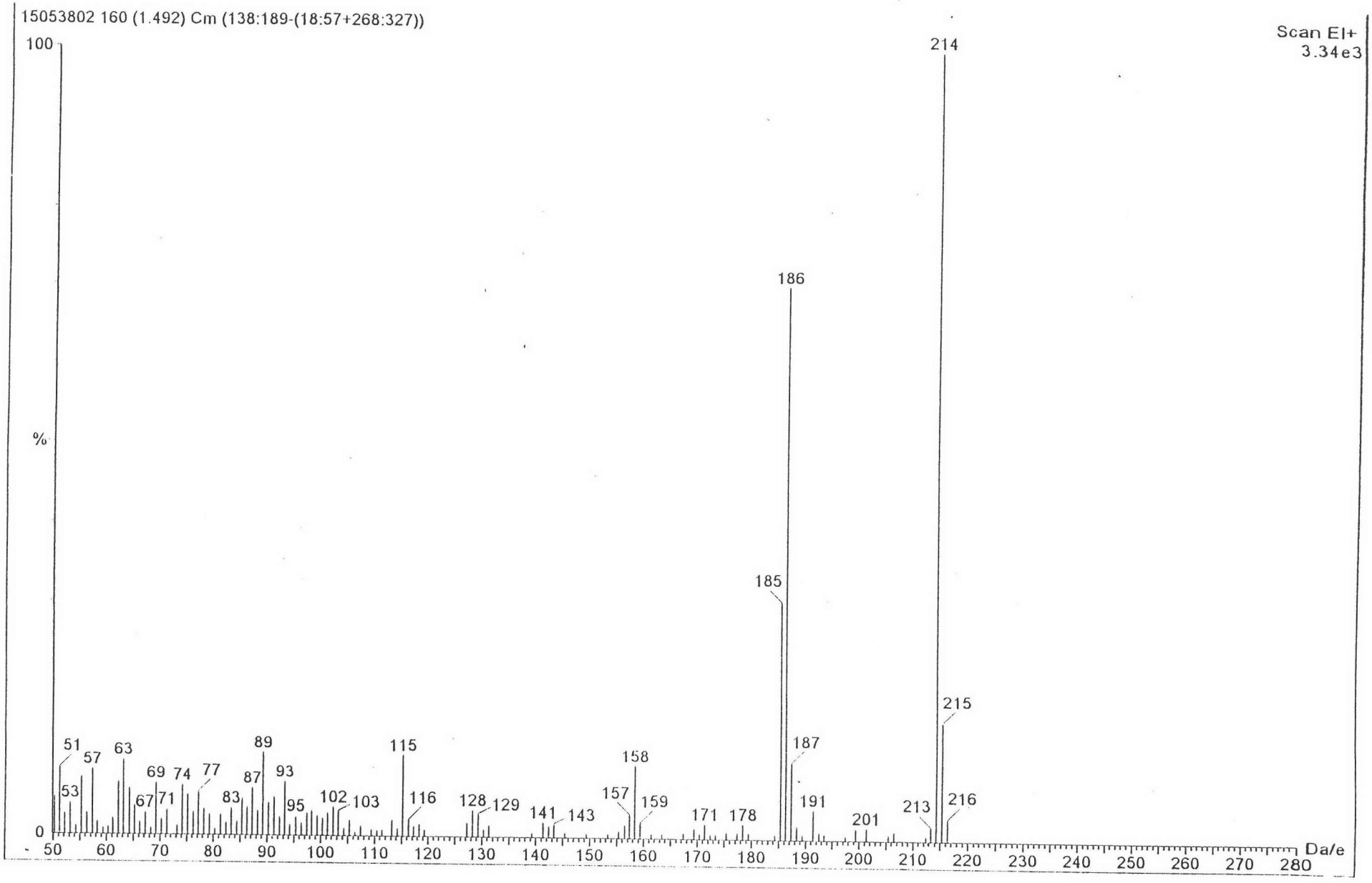

Figure 8 : Mass spectrum of anhydrobarakol hydrochloride.

384 (4.29) (Figure 9); IR ν_{max} (KBr) 3046, 1667, 1564 and 1527 cm^{-1} (Figure 10); ^{1}H-NMR ($CDCl_3$) : δ 6.69 (1H,d) 6.16 (1H,d), 2.49 (3H,s), 2.33 (3H,d) (Figure 11). MS, m/z (rel.): M^+ 467 (14.8), 466 (100), 438 (10), 339 (11), 311 (16), 184 (12), 169 (13) and 43 (17) (Figure 12). The melting point was identified at 220 ^{o}C (dec.) while the Rf value was shown at 0.24 when using the mixture of chloroform and ethyl acetate (6:4) as the mobile phase. These data were similar to those demonstrated by the previous works of Kaokaew (1993) (Table 3). The yield of the products are 50 percent.

3. Preparation of [^{125}I]anhydrobarakol hydrochloride

3.1. Preparation of chloramine-T , sodium iodide, [I]anhydrobarakol hydrochloride complex and anhydrobarakol hydrochloride standard.

Standard peaks of chloramine-T, sodium iodide, [I]anhydrobarakol hydrochloride complex and anhydrobarakol hydrochloride, obtained from the HPLC when using the solvent system containing acetronitrile: distilled water (70:30, flow rate 1 ml/min) were demonstrated as sharp single peak with retention time 2.692 (Figure 13), 2.280 (Figure 14), 4.301 (Figure 15) and 5.776 minute respectively (Figure 16).

3.2 Preparation of [I]anhydrobarakol hydrochloride in microscales.

Yellow brown solution obtained from the reaction in microscale was mixed with solvent consisting of acetronitrile and distilled water (70:30). Then, 60 µl of the mixture was injected into the HPLC which demonstrated profiles with four main sharp

Table 3 Spectroscopic characteristics of [I]anhydrobarakol hydrochloride.

Type of spectrum	[I]Anhydrobarakol hydrochloride (Kaokeaw,1993)	[I]Anhydrobarakol hydrochloride (Present study)
UV λ_{MAX} nm (log ε)	in EtOH 258(4.8), 397(4.33)	in EtOH 246(4.87), 384(4.29)
IR ν_{max} (cm^{-1})	in KBr 3030, 1664, 1565, 1529	in KBr 3046, 1667, 1564, 1527
NMR δ value (ppm)	in $CDCl_3$ 6.69(1H,s), 6,17 (1H,s), 2.52, 2.30(6H,d)	in $CDCl_3$ 6.69(1H,d), 6.16(1H,d), 2.49(3H,s),2.33(3H,d)
Mass spectra (m/z)	M^+ 467(14.8), 466(100),438(9), 439(17), 311(15), 184(13), 169(12), 43(18)	M^+ 467(14.8), 466(100), 438(10), 339(11), 311(16), 184(12), 169(13), 43(17)

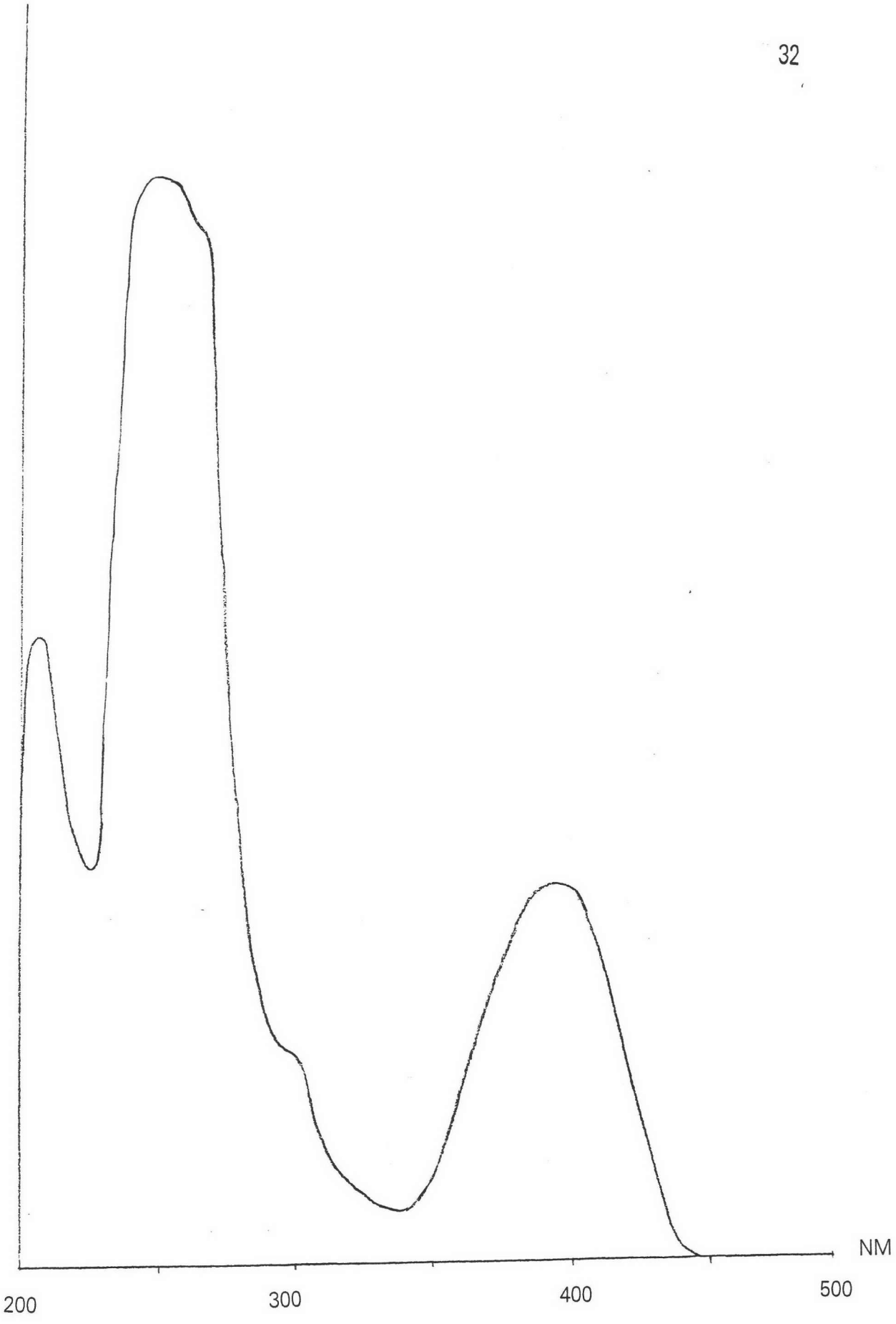

Figure 9 : UV absorption spectrum of [I]anhydrobarakol hydrochloride, in ethanol.

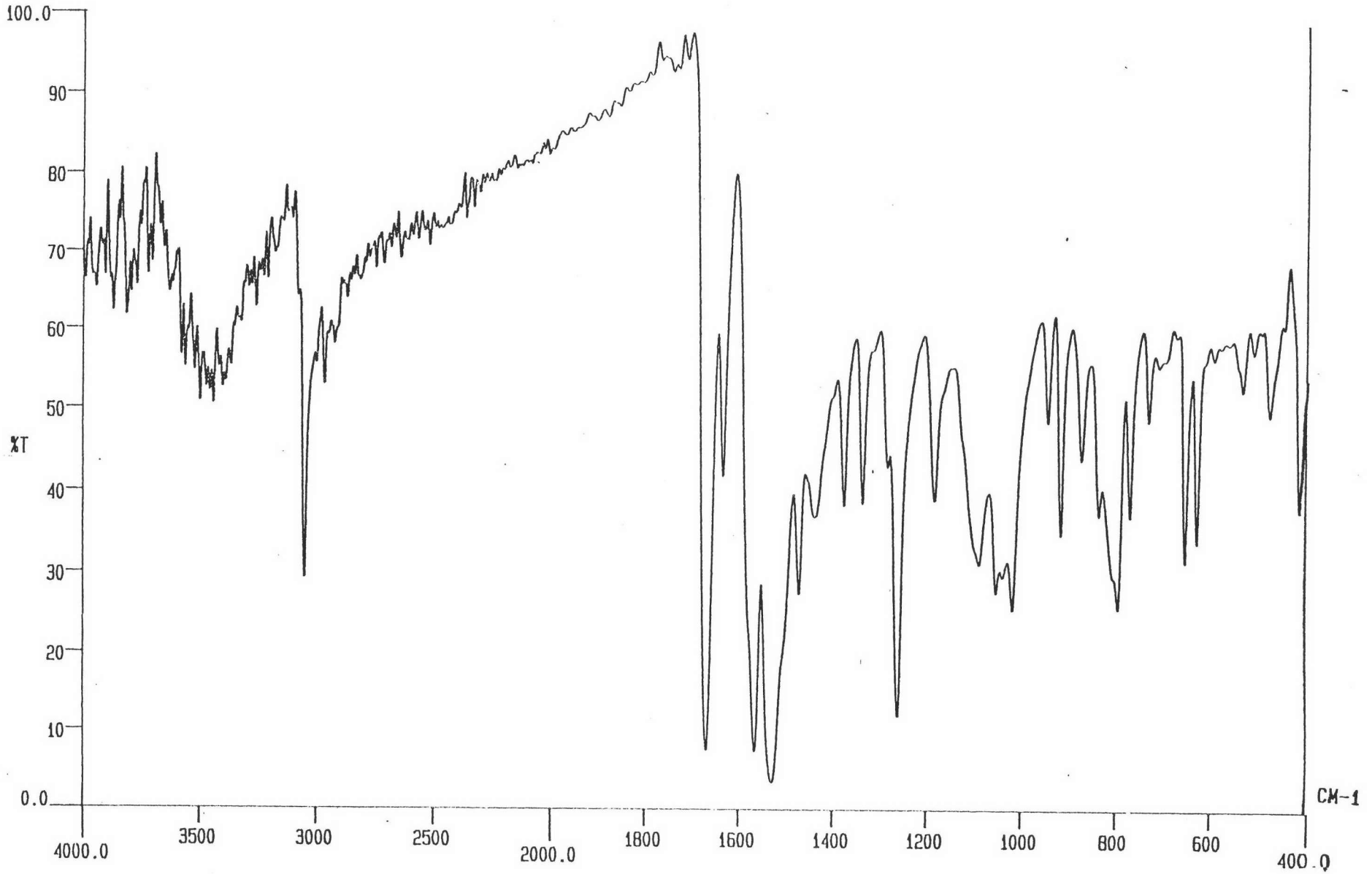

Figure 10 : IR absorption spectrum of [I]anhydrobarakol hydrochloride, in KBr.

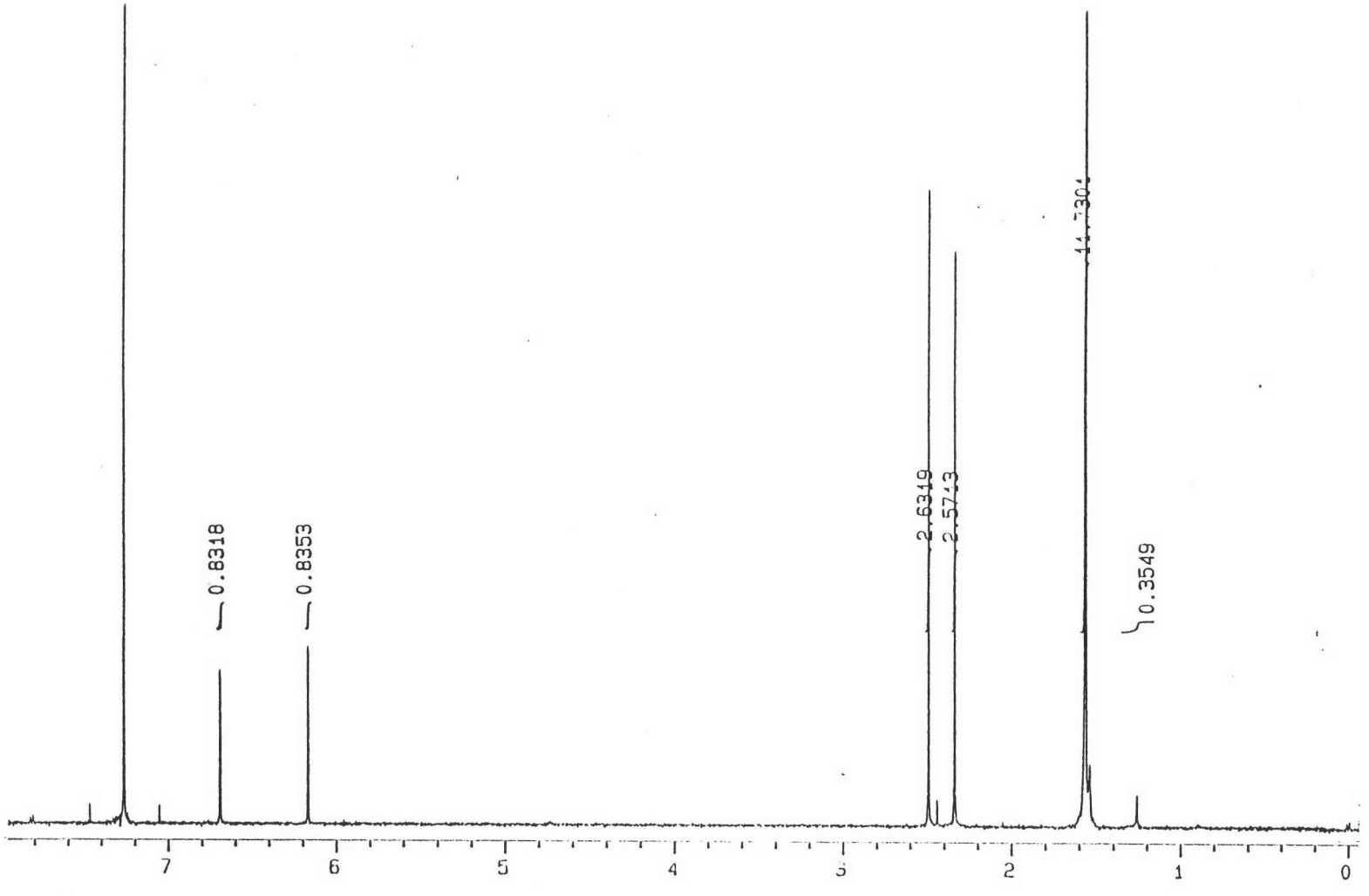

Figure 11 : ^{1}H NMR spectrum of [I]anhydrabarakol hydrochloride, in $CDCl_3$ (at 200 MHz).

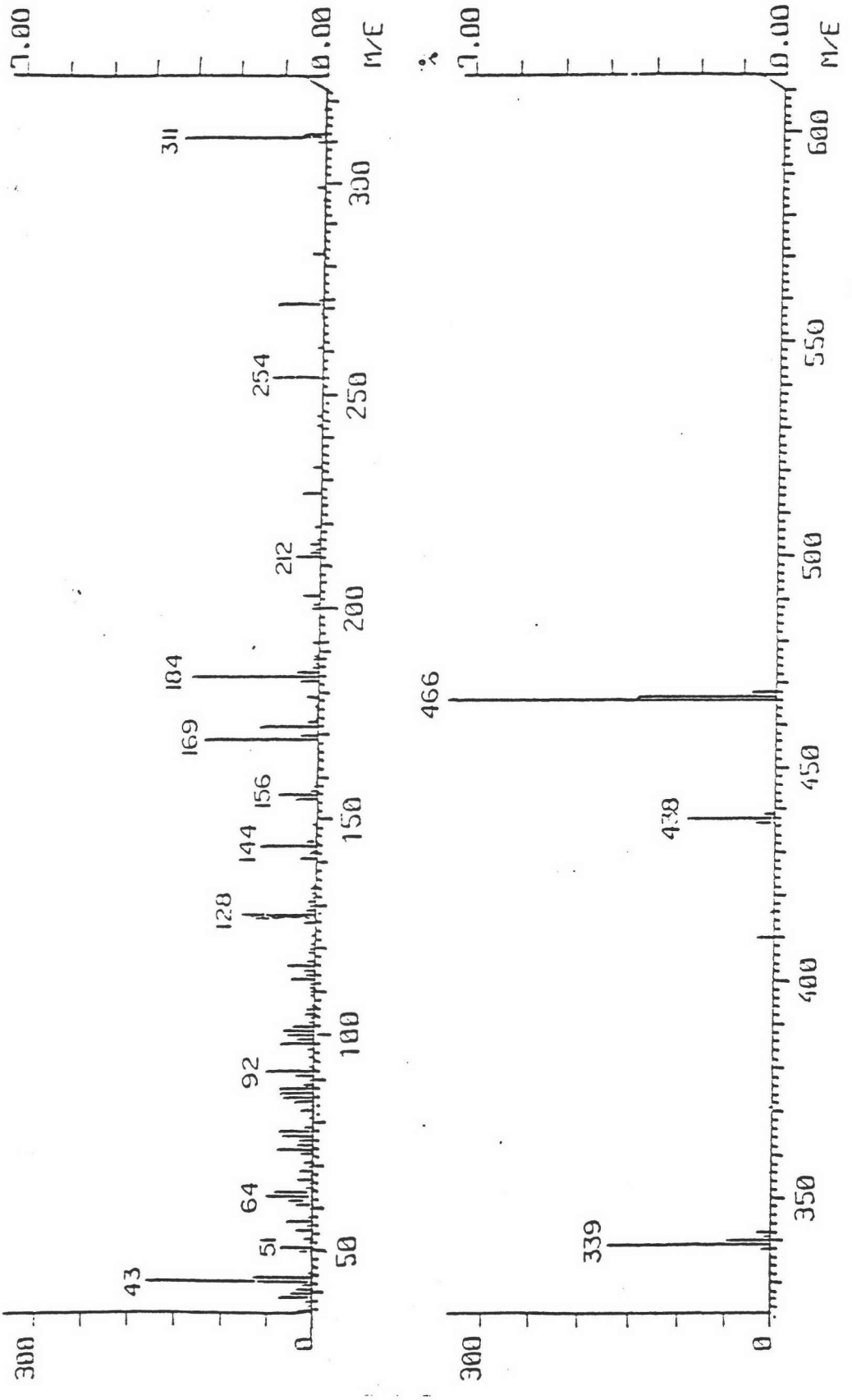

Figure 12 : Mass spectrum of Illanhydrobarakol hydrochloride.

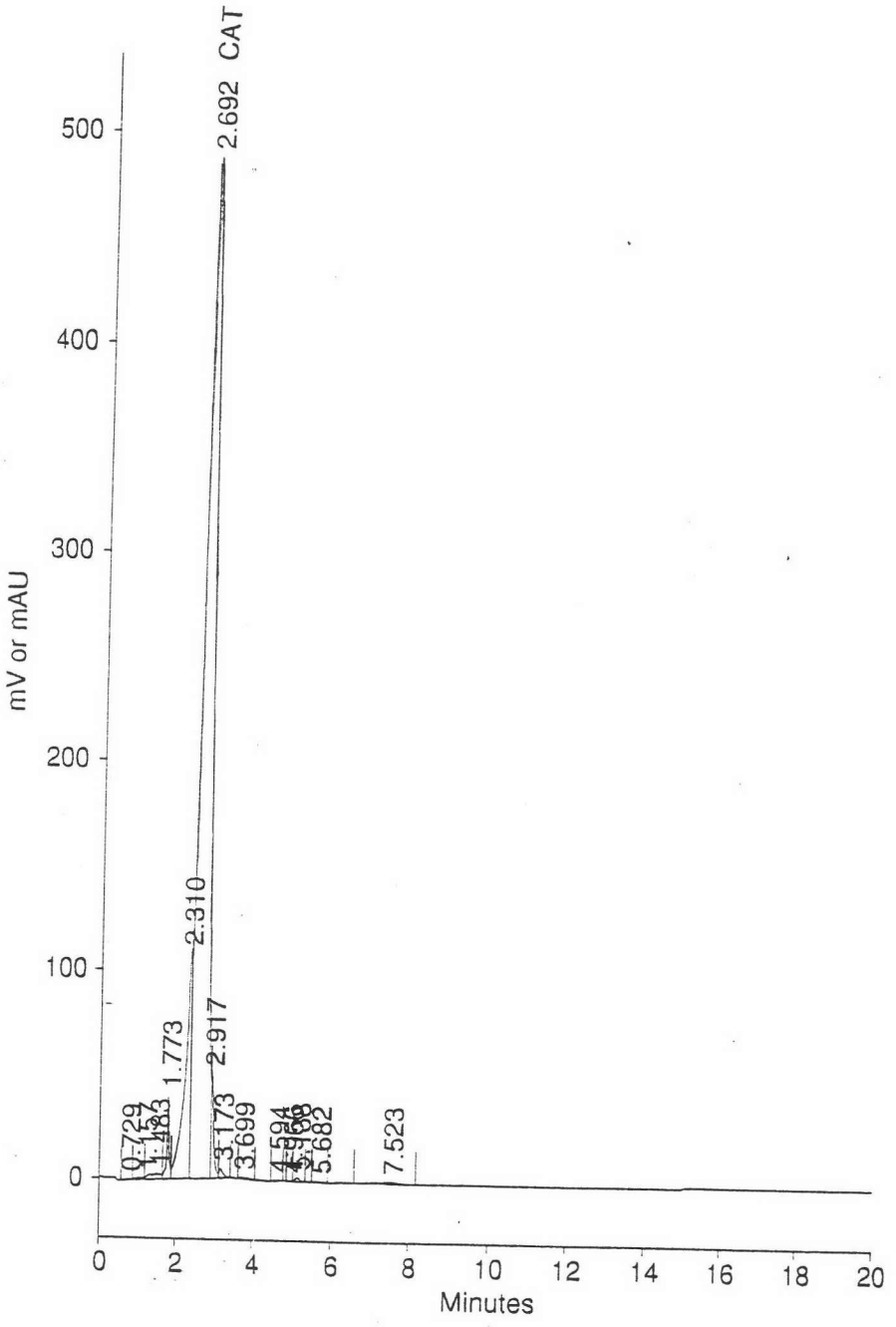

Figure 13 : Representative HPLC profiles of chloramine-T standard.

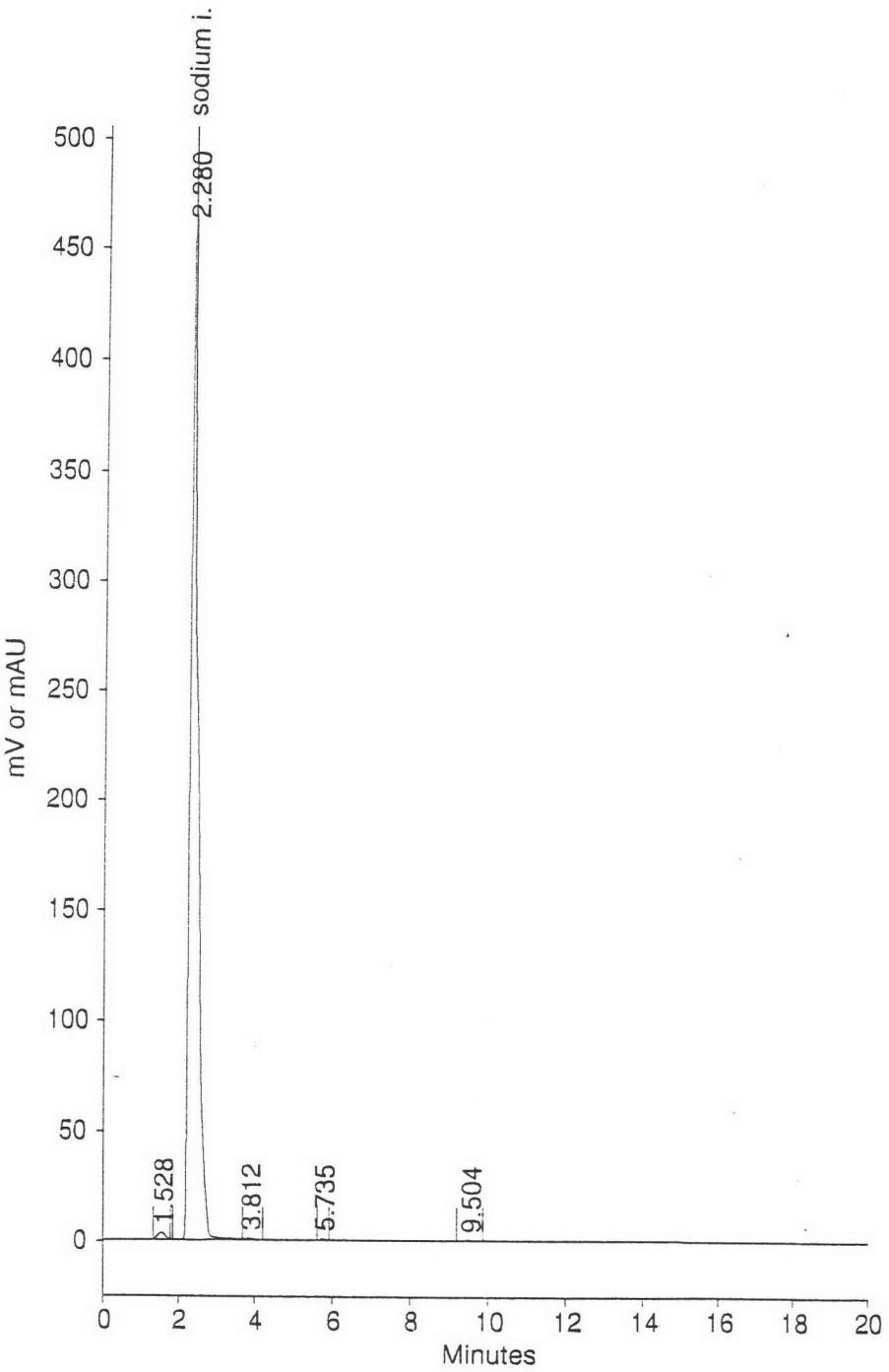

Figure 14 : Representative HPLC profiles of sodium iodide standard.

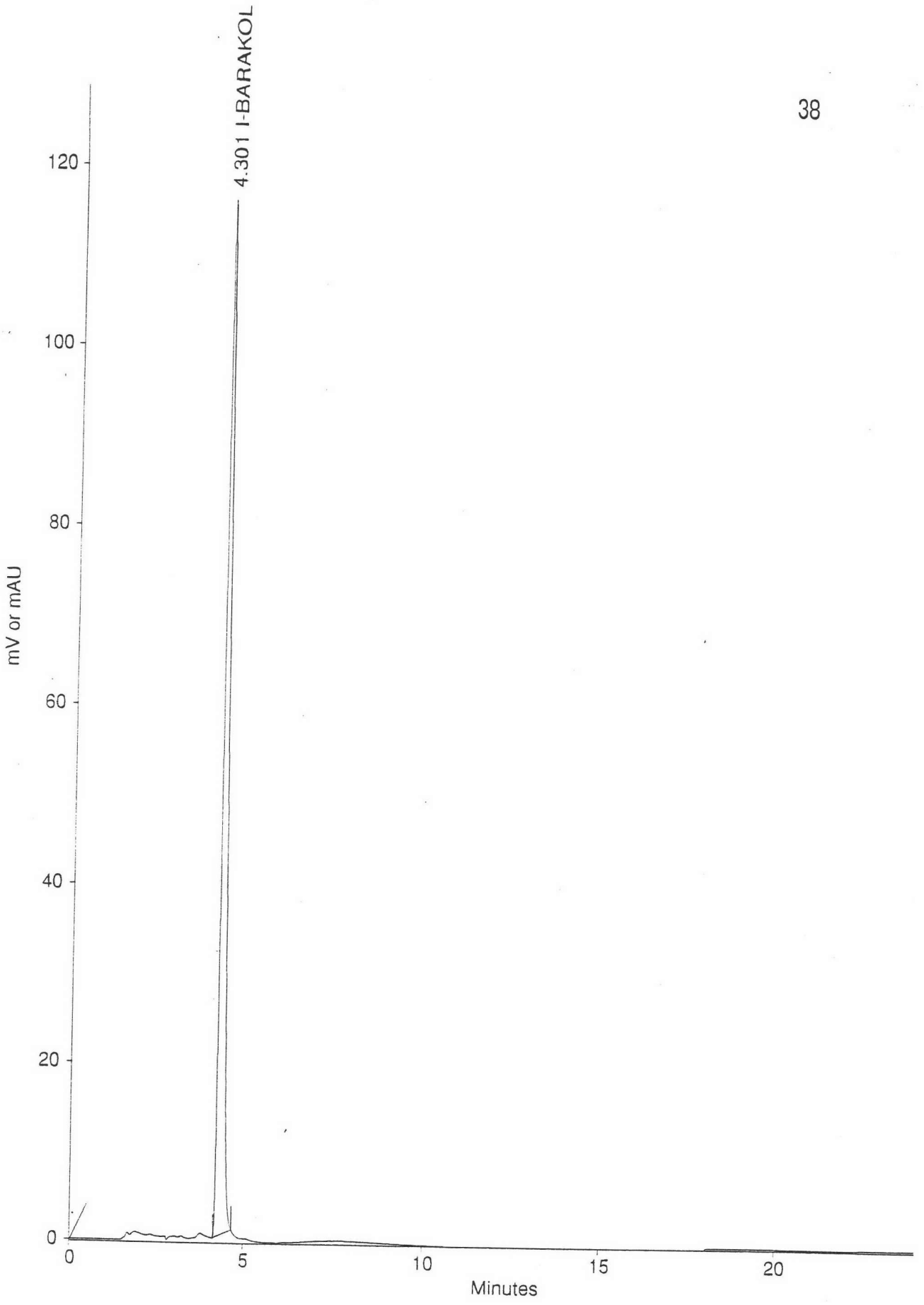

Figure 15 : Representative HPLC profiles of [I]anhydrobarakol hydrochloride complex standard.

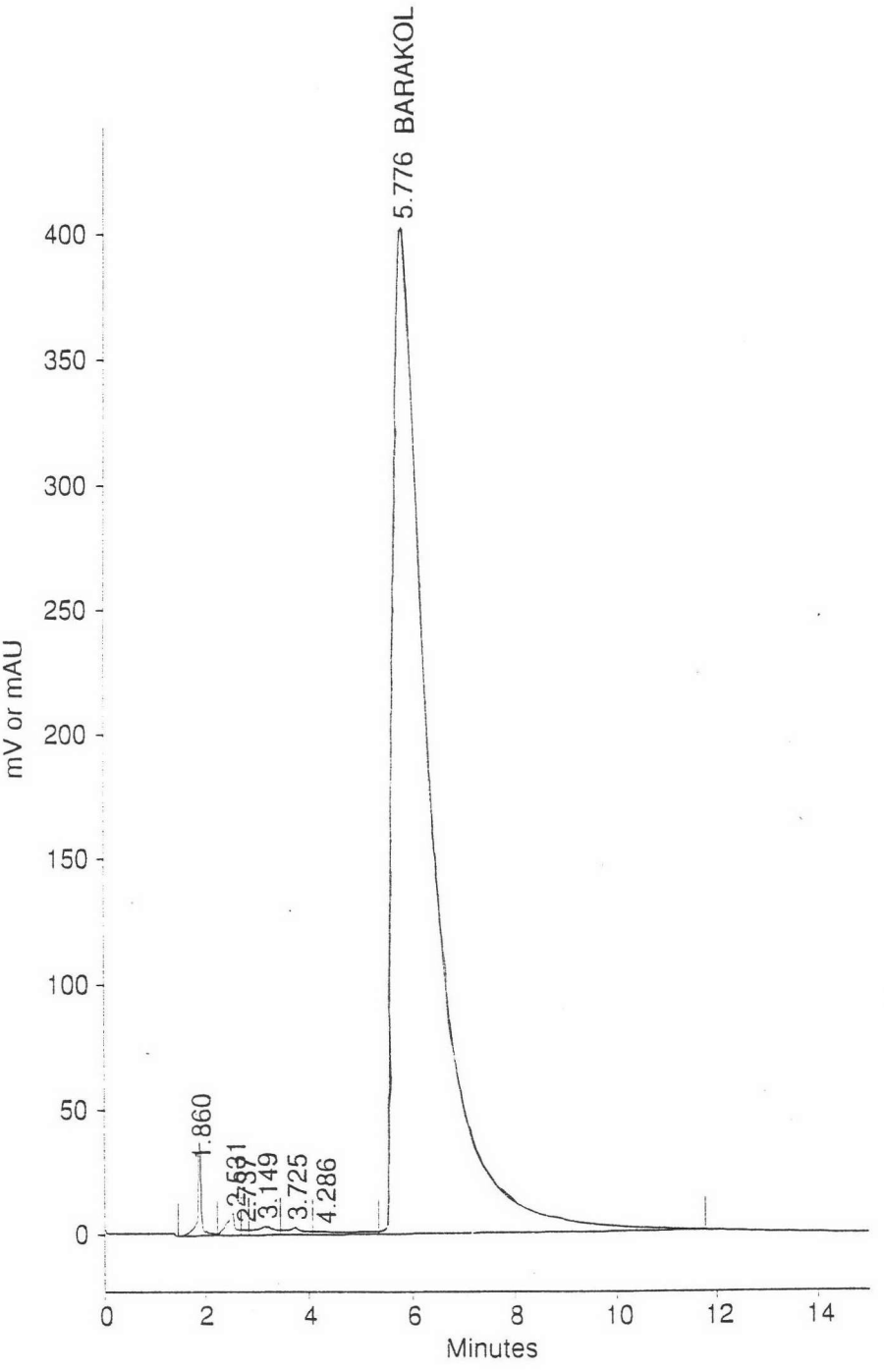

Figure 16 : Representative HPLC profiles of anhydrobarakol hydrochloride standard.

peaks. The retention time of the peaks were measured at 2.608, 3.714, 4.297, and 5.994 minutes postinjection respectively (Figure 17).

3.3 Confirmation of the [I]anhydrobarakol hydrochloride by HPLC

Iodination reaction obtained from 3.2 was added with 60 µl of standard anhydrobarakol hydrochloride (1mg/ml) prior to injected into the HPLC. The HPLC profiles was demonstrated a sharply increase of only the peak at retention time 4.307 minute (Figure 18).

3.4 Preparation of [^{125}I]anhydrobarakol hydrochloride

The preparation of [^{125}I]anhydrobarakol hydrochloride compound were prepared as in 3.2 by using sodium iodide-125 [Na^{125}I] instead of sodium iodide [NaI].The solution was mixed with the solvent (acetronitrite and distilled water, 70:30) prior injected into HPLC. Collections of solutions were undertaken only the peaks with retention time 2.318, 3.710, 4.275, and 5.716 minute postinjection (Figure 19) and measured radioactivity of each fraction by gamma counter. It was found that very high radioactivity ranging between 30,000-40,000 count per second was shown in the fraction of the peak at retention time 4.275 minute.

4. Demonstration and localization of [^{125}I]anhydrobarakol hydrochloride binding sites in rat brains by in vitro receptor autoradiography.

Fraction at retention time 4.275 minute collected from the HPLC was used as radioligand for demonstration and localization of the binding sites of anhydrobarakol hydrochloride. This fraction contain the [^{125}I]anhydrobarakol hydrochloride since its peak

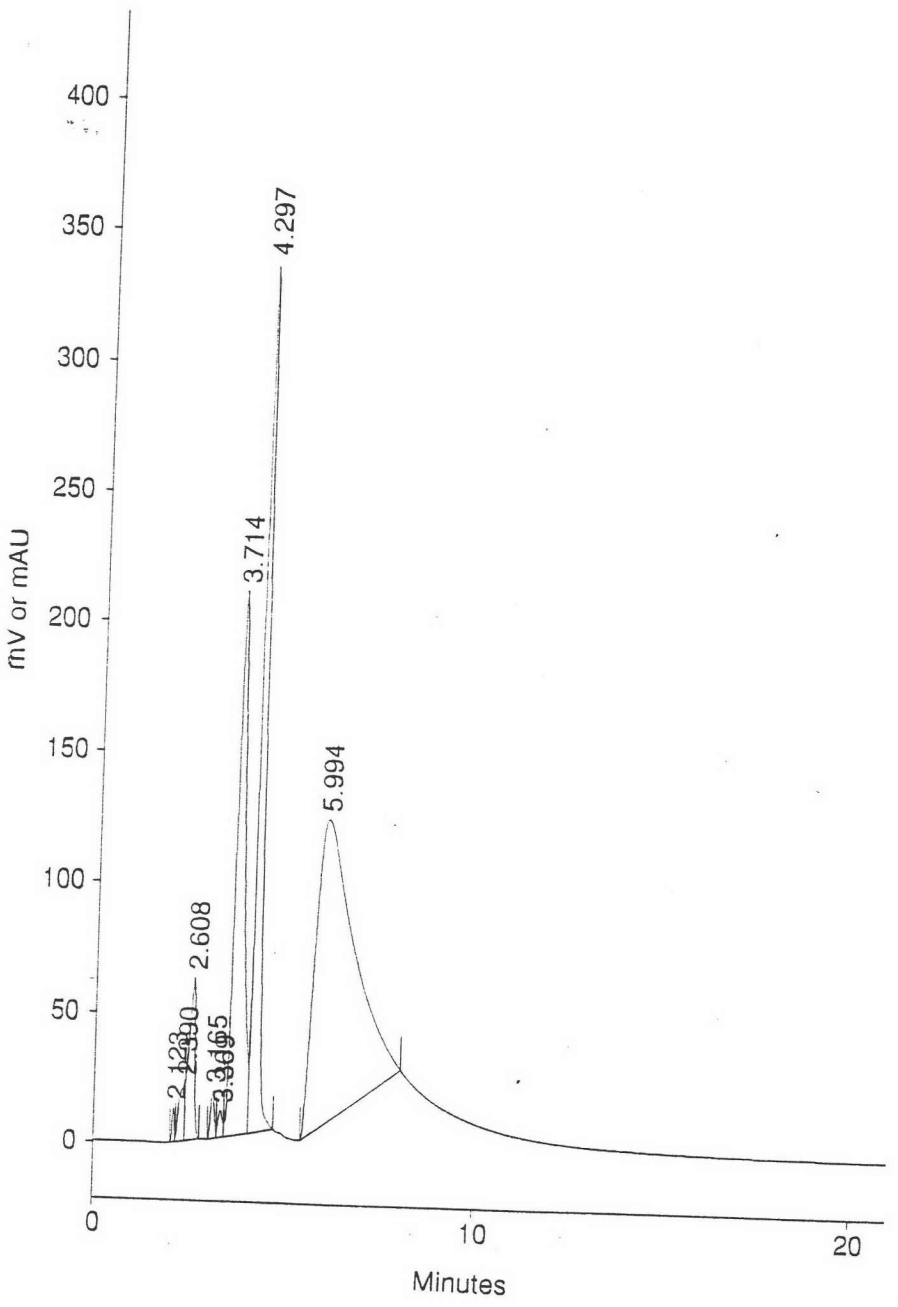

Figure 17 : Representative HPLC profiles after injection of solution obtained from iodination reaction.

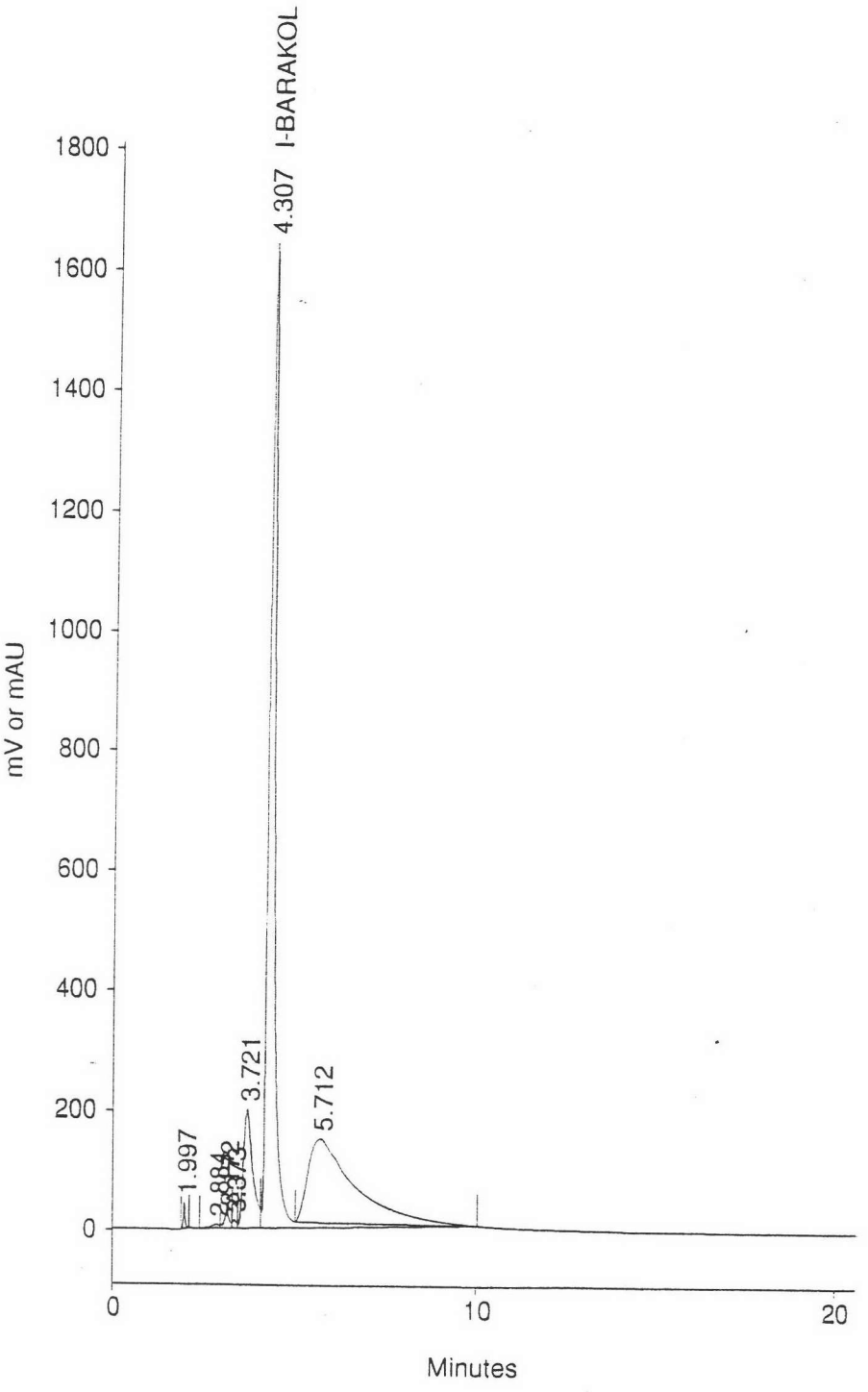

Figure 18 : Representative HPLC profiles of [I]anhydrobarakol hydrochloride after added with [I]anhydrobarakol hydrochloride from column chromatography.

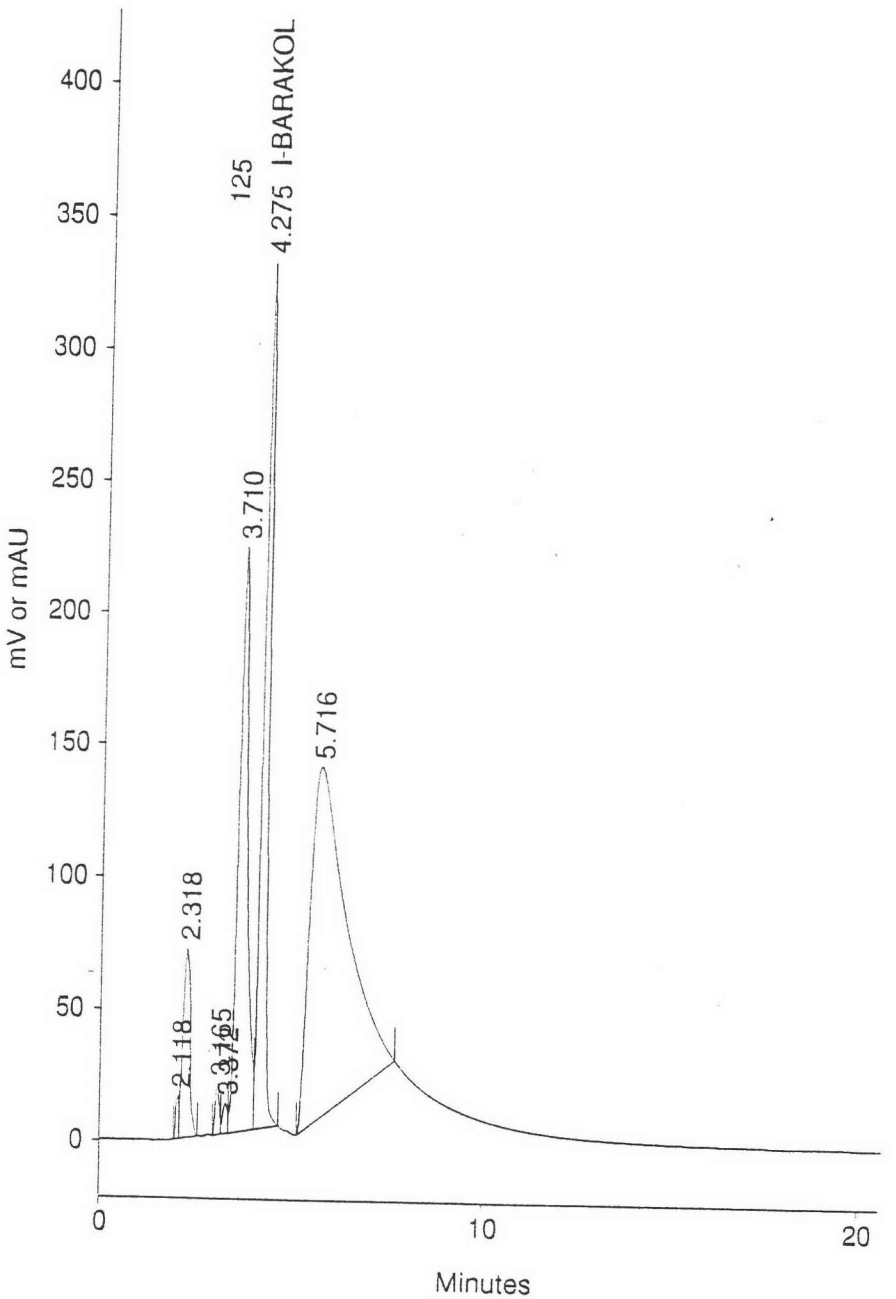

Figure 19 : Representative HPLC profiles of iodinated reaction of [^{125}I] anhydrobarakol hydrochloride.

corresponded to the standard in 3.2 and reconfirmed by having very close retention time of spike peak in 3.3.

Distribution of [^{125}I]anhydrobarakol hydrochloride binding sites in rat brains were consistent. The specific binding sites of [^{125}I]anhydrobarakol hydrochloride were found in the caudate putamen, accumben nucleus, cerebral cortex, hippocampus, thalamic nucleus, granule cell layer of cerebellum, inferior colliculus and substantia nigra.

High grain density was demonstrated on the Hyperfilm at various area of the brain after employing the radioligand at concentration 10^{-7} M. This grain density abruptly decrease to the level of background density after the tissues were co-incubated with cold ligand (anhydrobarakol hydrochloride) at concentration 10^{-3} M.

Medium grain density was clearly observed in a whole caudate putamen nucleus from the rostral level until the level of rostral part of thalamic nucleus (figure 20,22). The grain density was also observed in the nucleus accumben (Figure 20).

High grain density was observed in the cortex from the level of frontoparietal cortex,motor and somatosensory area (Figure 20, 22, 24) to the level of striate cortex and entorhinal cortex (Figure 28, 29). In thalamic nucleus, high grain density was observed from the rostral to the caudal level (Figure 24).

High grain density was clearly observed in the ventral hippocampus while medium grain density was observed in the dorsal hippocampus (Figure 26).

In cerebellum, high grain density was observed only in the granular cell layer along its entire length (Figure 29, 31, 33).

In mesencephalon, medium grain density was observed in the substantia nigra (Figure 26) and inferior colliculus (Figure 29).

The addition of [I]anhydrobarakol hydrochloride resulted in a marked reduction in labeling of binding sites in caudate putamen (Figure 21), hippocampus (Figure 27), cerebellum (Figure 21), cerebral cortex (Figure 21, 23, 27), mesencephalic areas (Figure 27), and thalamus (Figure 25).

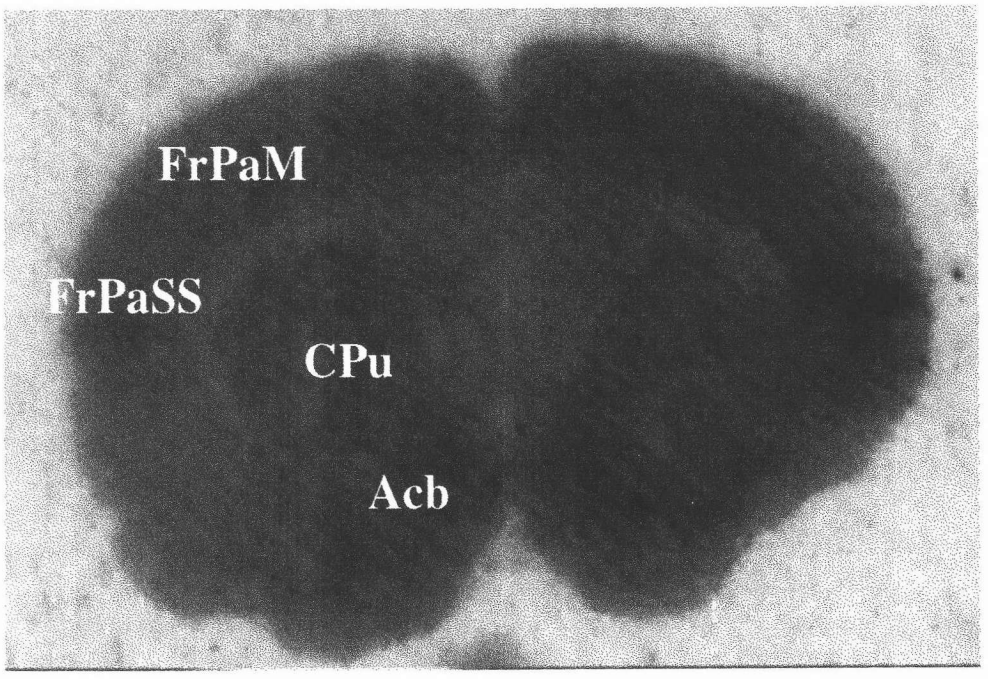

Figure 20 : Total binding sites of [^{125}I]anhydrobarakol hydrobarakol hydrochloride in caudate-putamen (CPu), accumben nucleus (Acb), frontoparietal cortex-motor area (FrPaM), and frontoparietal cortex-somatosensory area (FrPaSS) in rat brain.

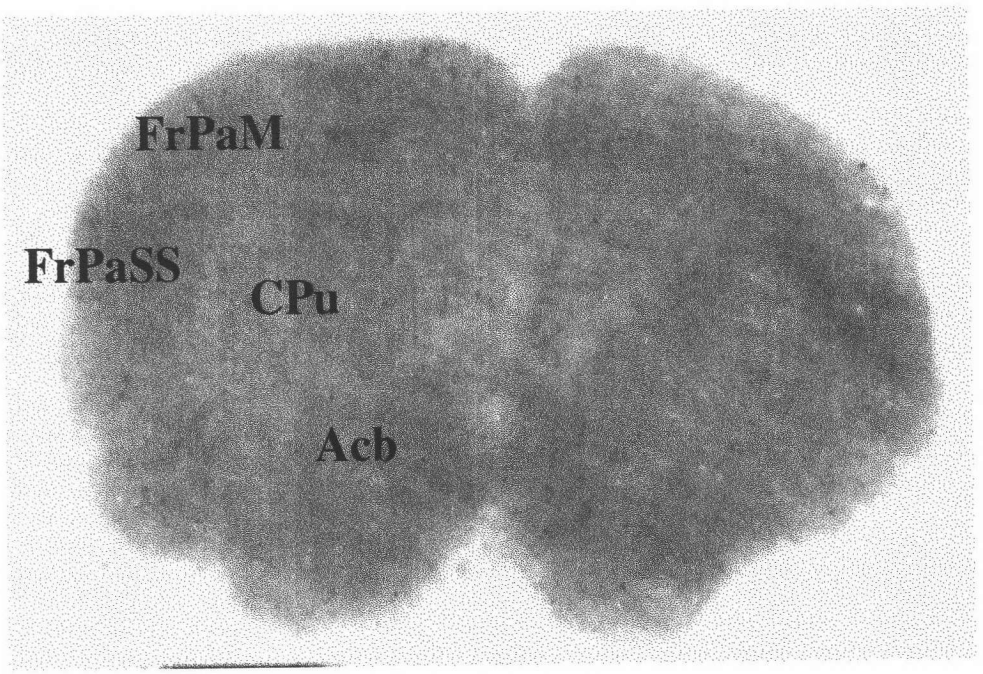

Figure 21 : Non-specific binding sites of [^{125}I]anhydrobarakol hydrobarakol hydrochloride in caudate-putamen (CPu), accumben nucleus (Acb), frontoparietal cortex-motor area (FrPaM), and frontoparietal cortex-somatosensory area (FrPaSS) in adjacent section of rat brain.

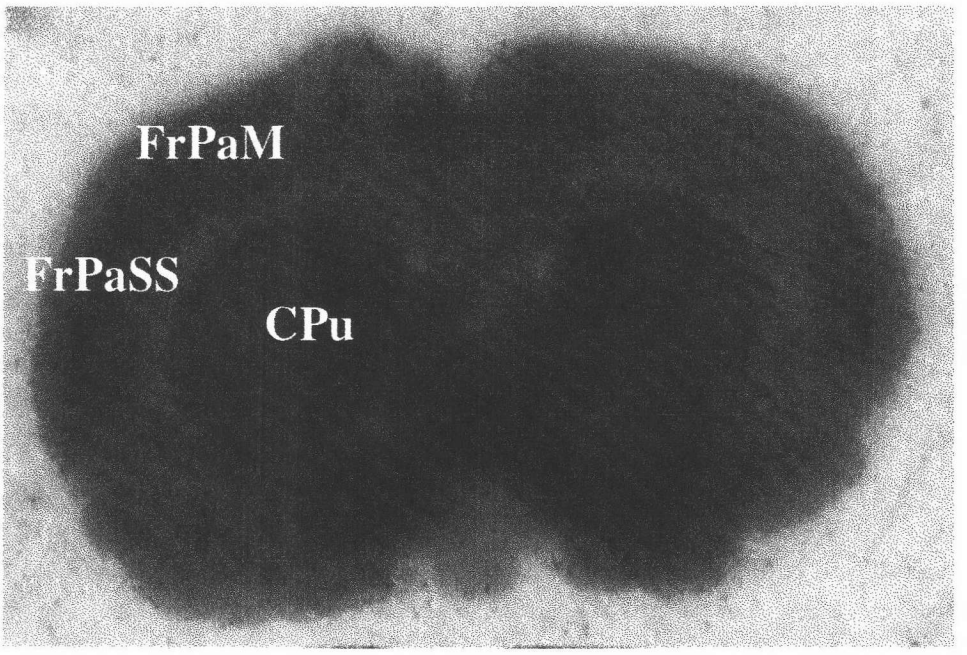

Figure 22 : Total binding sites of [^{125}I]anhydrobarakol hydrochloride in caudate-putamen (CPu), frontoparietal cortex-motor area (FrPaM), and frontoparietal cortex -somatosensory area (FrPaSS) of rat brain.

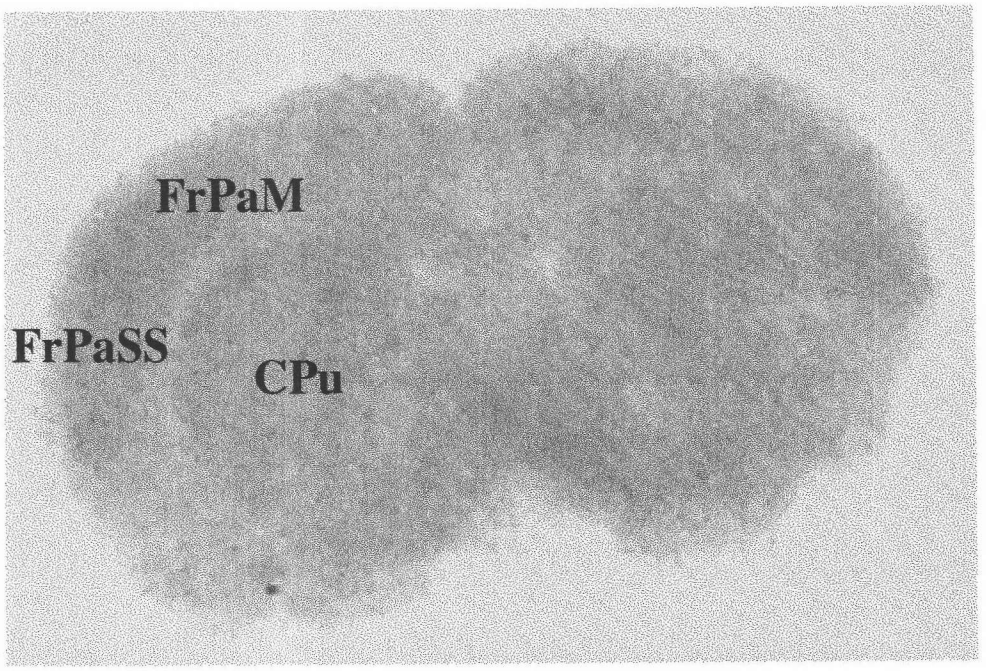

Figure 23 : Non-specific binding sites of [^{125}I]anhydrobarakol hydrochloride in caudate-putamen (CPu), frontoparietal cortex-motor area (FrPaM), and frontoparietal cortex-somatosensory area (FrPaSS) in adjacent section of rat brain.

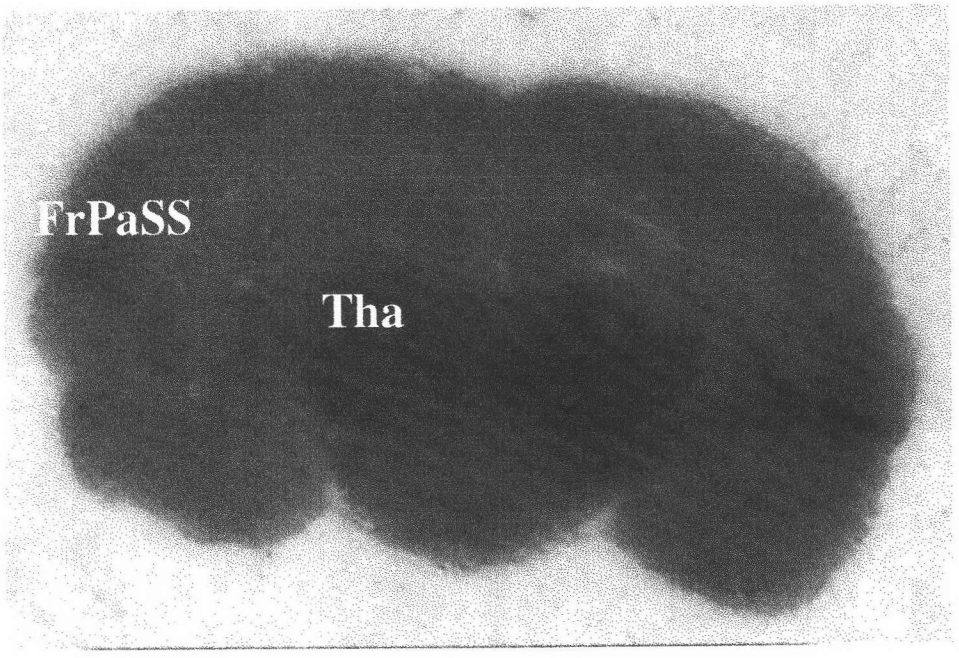

Figure 24 : Total binding sites of [^{125}I]anhydrobarakol hydrochloride in frontoparietal cortex-somatosensory area (FrPaSS) and thalamic nucleus (Tha) of rat brain.

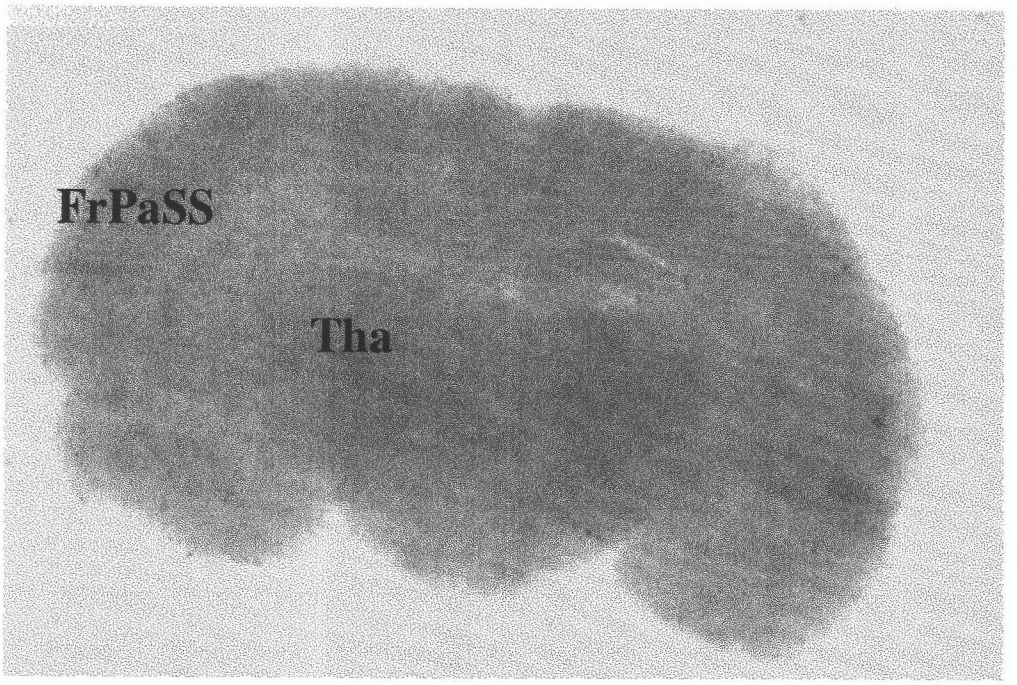

Figure 25 : Non-specific binding sites of [^{125}I]anhydrobarakol hydrochloride in frontoparietal cortex-somatosensory area (FrPaSS), thalamic nucleus (Tha) in adjacent sections of rat brain.

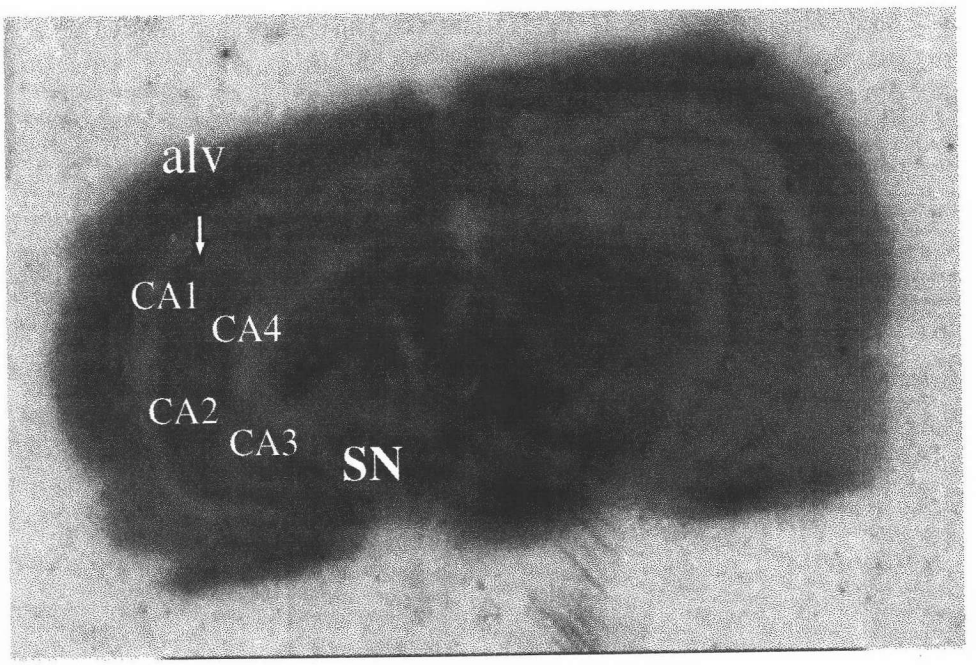

Figure 26 : Total binding sites of [^{125}I]anhydrobarakol hydrochloride in substantia nigra (SN) included pars compacta (SNC) and pars reticulata (SNR), in ventral hippocampus included field CA 1, CA 2, CA 3, and CA 4 of rat brain.

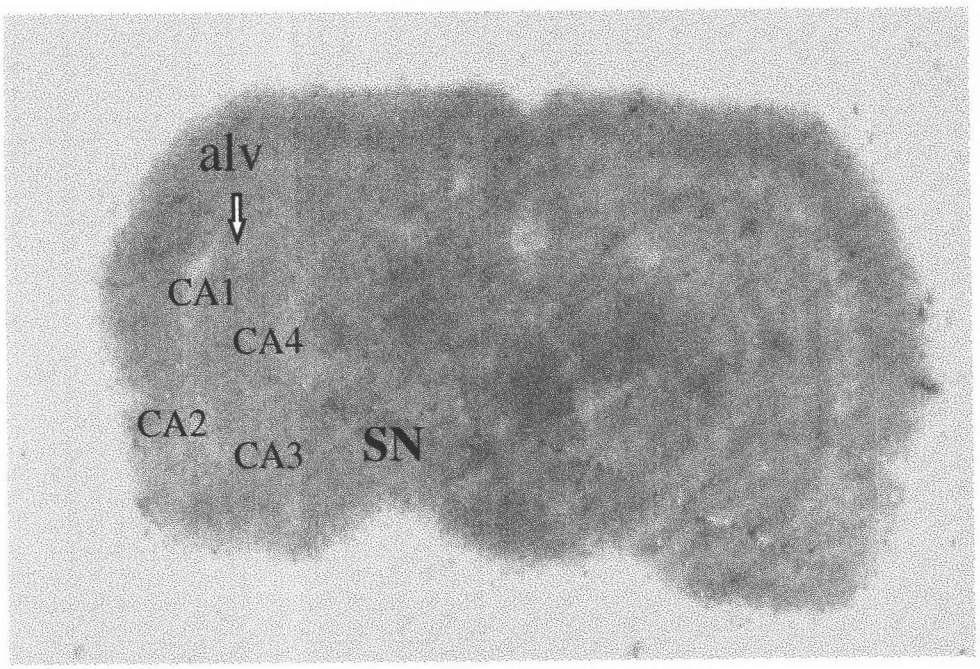

Figure 27 : Non-specific binding sites of [^{125}I]anhydrobarakol hydrochloride in substantia nigra (SN) included pars compacta (SNC) and pars reticulata (SNR), in ventral hippocampus in adjacent sections of rat brain.

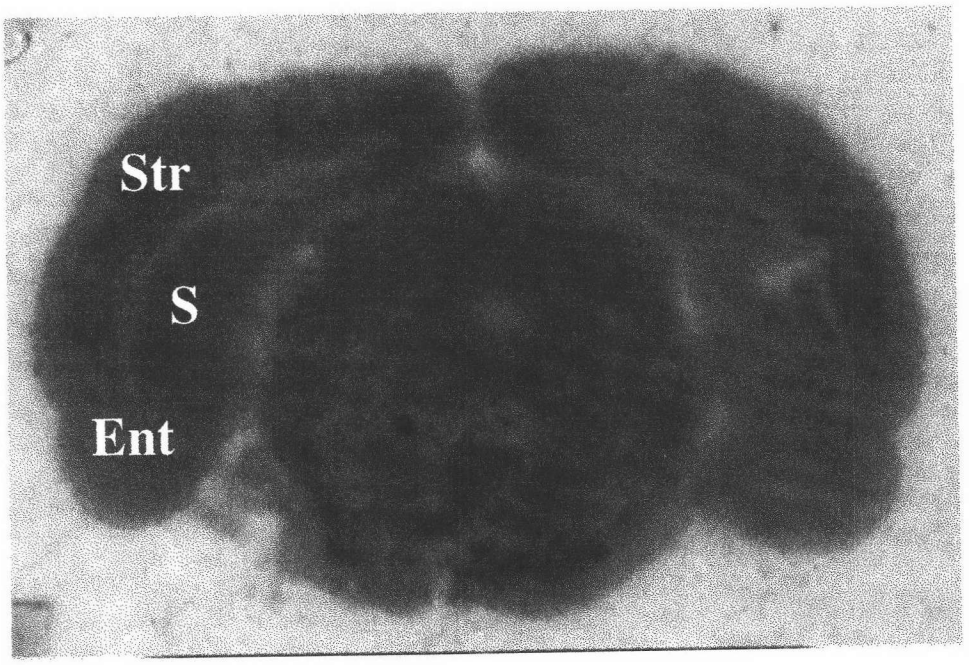

Figure 28 : Total binding sites of [^{125}I]anhydrobarakol hydrochloride in striate cortex (Str), subiculum (S) and entorhinal cortex (Ent) of rat brain.

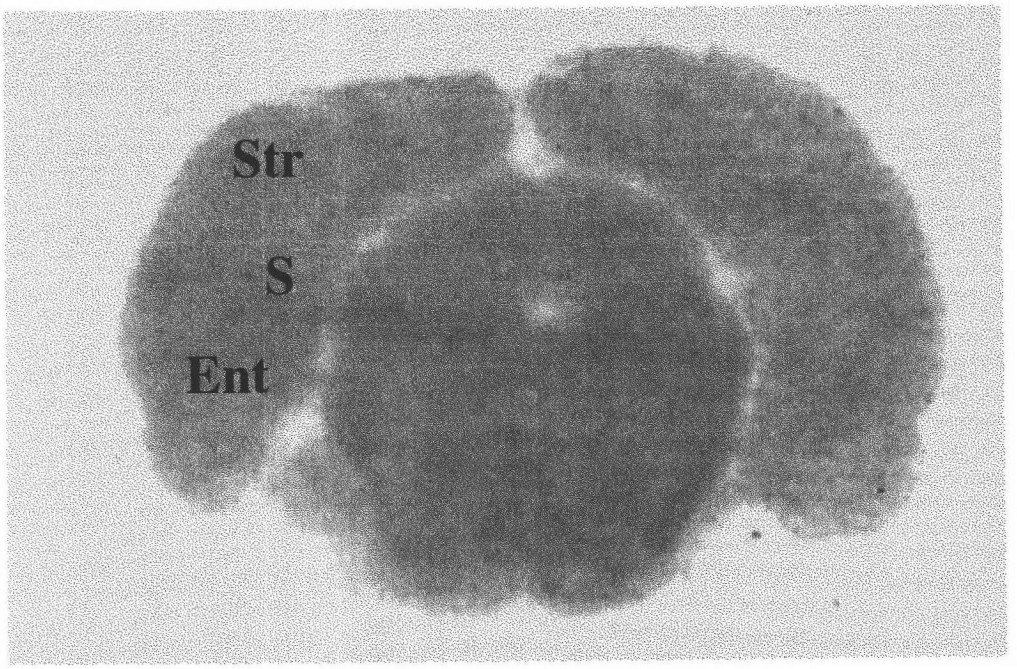

Figure 29 : Non-specific binding sites of [^{125}I]anhydrobarakol hydrochloride in striate cortex (Str), subiculum (S) and entorhinal cortex (Ent) in adjasent section of rat brain.

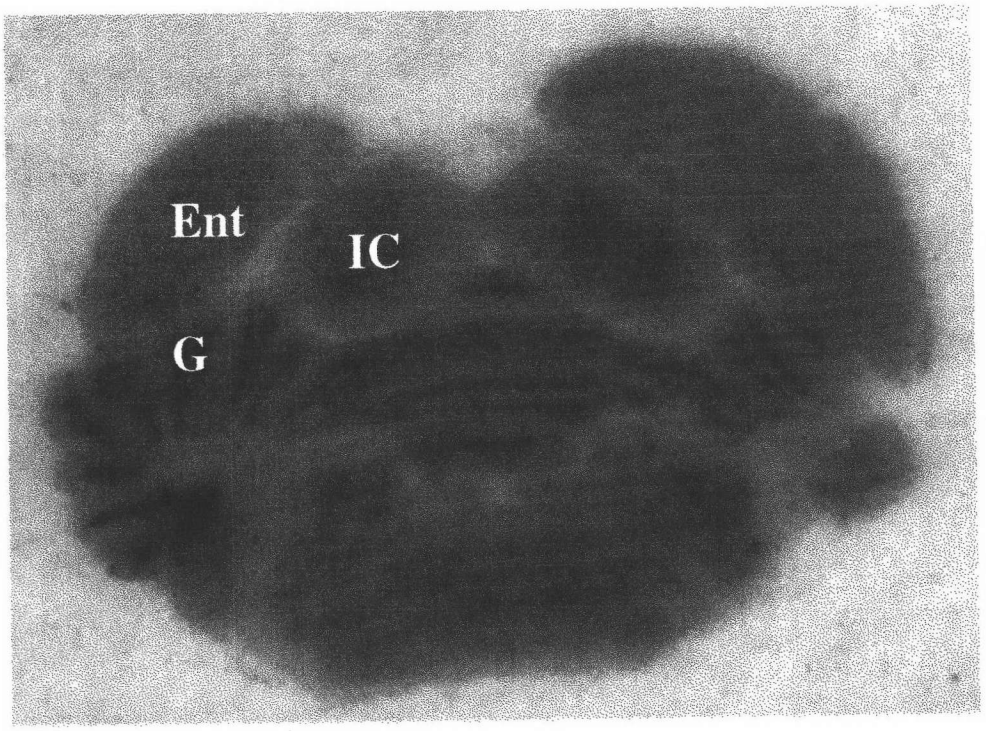

Figure 30 : Total binding sites of [^{125}I]anhydrobarakol hydrochloride in inferior colliculus (IC), granular cell layer of cerebellum (G) and entorhinal cortex (Ent) of rat brain.

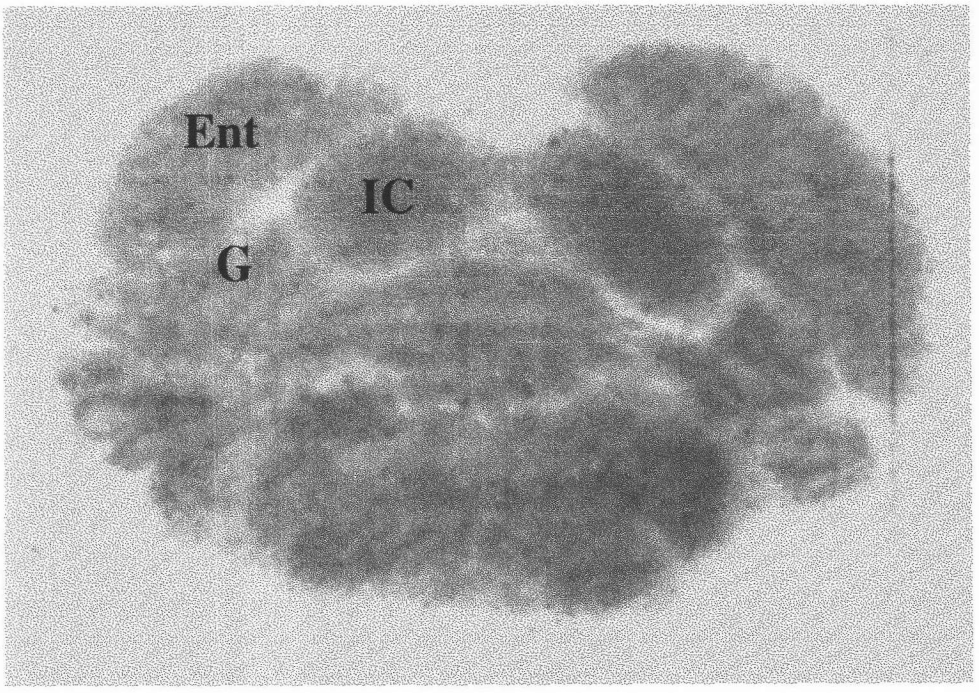

Figure 31 : Non-specific binding sites of [^{125}I]anhydrobarakol hydrochloride in inferior colliculus (IC), granule cell layer of cerebellum (G) and entorhinal cortex (Ent) in adjacent section of rat brain.

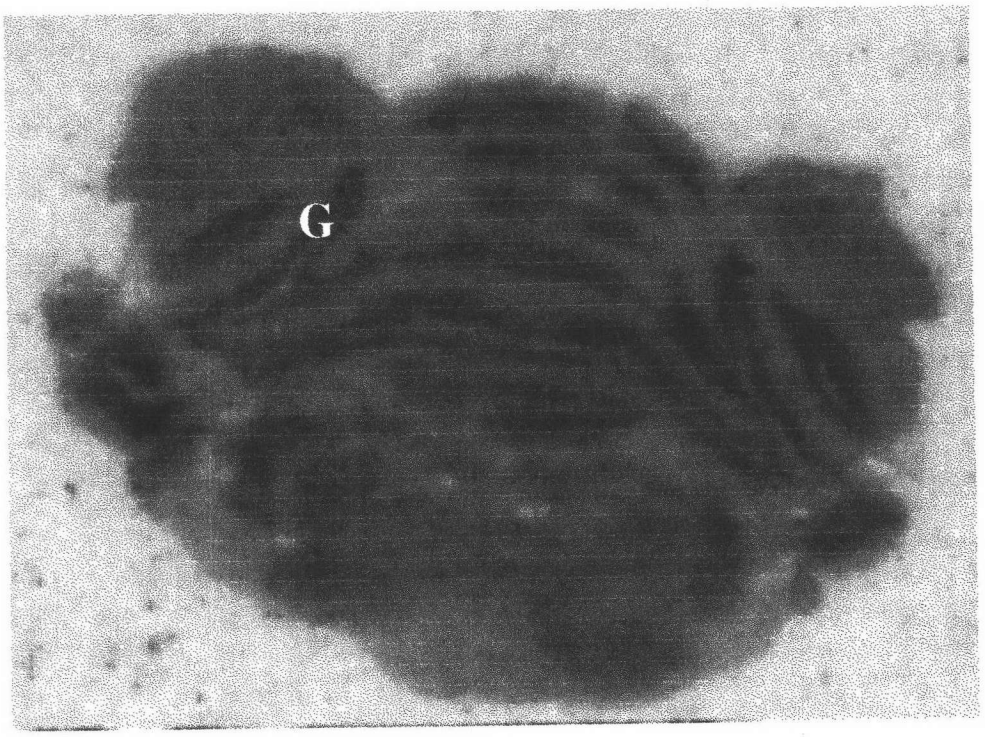

Figure 32 : Total binding sites of [^{125}I]anhydrobarakol hydrochloride in granular cell layer of cerebellum (G) of rat brain.

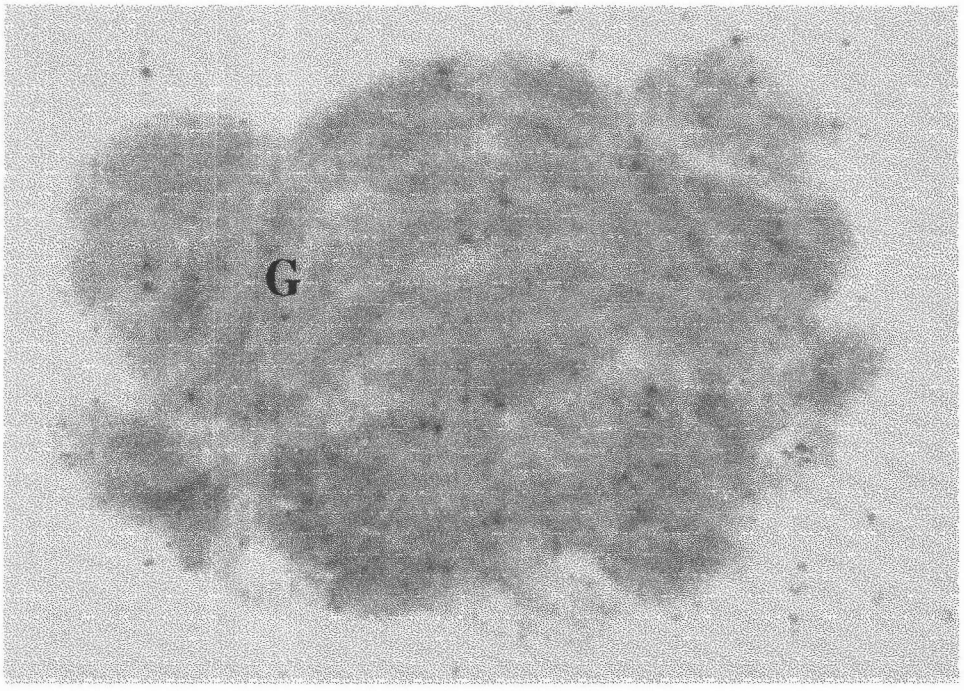

Figure 33 : Non-specific binding sites of [^{125}I]anhydrobarakol hydrochloride in granular cell layer of cerebellum (G), in adjacent section of rat brain.